15B.6 THE TORNADIC QUASI-LINEAR CONVECTIVE SYSTEM OVER EAST-CENTRAL WISCONSIN ON 6-7 AUGUST 2013. PART 2: RADAR AND MESOVORTEX ANALYSIS

Eugene S. Brusky* and Ashley Allen
NOAA/National Weather Service, Green Bay, WI
R.W. Przybylinski
NOAA/National Weather Service, St Louis, MO
E. Townsend Jr
NOAA/ National Weather Service
Fairbanks, AK

1. INTRODUCTION

A quasi-linear convective system (QLCS), raced across Wisconsin during the late night and early morning hours of August 6-7, 2013, producing wind damage and several tornadoes in the east-central part of the state. Hundreds of homes, businesses and farm buildings were damaged. Thousands of trees and power lines were downed, leaving tens of thousands of people without power. Two minor injuries were reported during the storm, both at a campground in Waupaca County. Six tornadoes (5 EF-1 and 1 EF-2) were spawned during this event, all occurring within about a 45-minute period beginning at 1230 am CDT August 7 (Fig. 1). Climatologically, the six tornadoes that occurred on this day ranked as the third largest single day and the largest early morning (midnight to 6 am) outbreak in northeast Wisconsin since 1950.

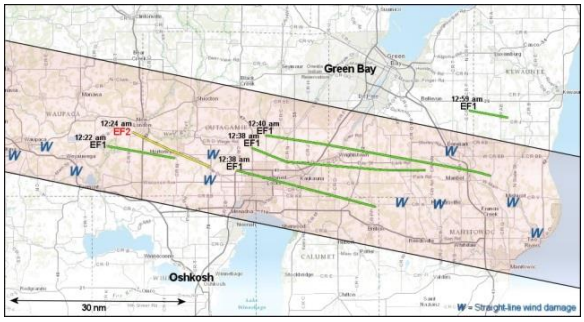

FIG.1. Tornado tracks (solid lines). Straight-tine wind damage (W).

2. PURPOSE OF THIS STUDY

In addition to the fact that this was the largest early morning tornado outbreak in northeast Wisconsin in over 60 years, there were aspects of this event that presented both short-term forecast and warning decision challenges. From a short-term forecast perspective, although much of the forecast area was included in a slight risk for severe thunderstorms (Fig. 2), the tornado threat was not well anticipated. As the evening progressed, expectations were for weakening discrete upstream convection over eastern Minnesota to congeal, forming an organized cold pool and the development of a quasi-linear convective system that would propagate eastward across Wisconsin overnight. However, considerable uncertainty existed as to the impact continued nocturnal cooling and low-level stabilization would have on the damaging wind threat downstream. Kis and Straka (2009) have emphasized the forecast challenges associated with nocturnal environments in their nocturnal tornado climatology study. A Severe Thunderstorm Watch was eventually issued later in the evening with large hail and sporadic straight-line wind damage the primary threats.

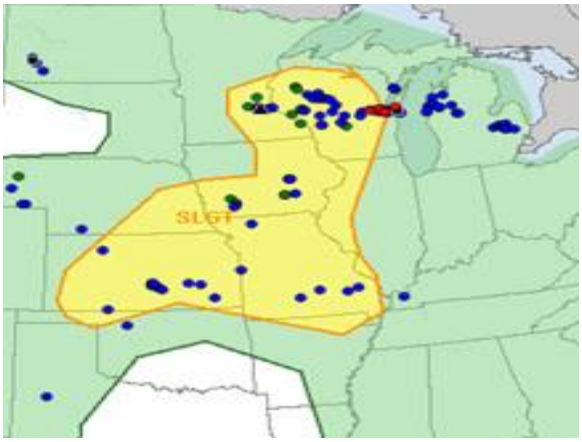

FIG. 2. Storm Prediction Center (SPC) 7 August 2013 01Z Convective Outlook and preliminary storm reports. Red dots denote tornado reports.

Doppler radar analysis and damage survey information indicated that all the tornadoes were associated with rapidly evolving mesovortices (MVs) observed along the leading edge of a bowing portion of the QLCS. Preliminary radar

* *Corresponding authors address:* Eugene S. Brusky, National Weather Service, 2485 South Point Road, Green Bay, WI 54313-5522; email: gene.brusky@noaa.gov

analysis indicated that the tornadic mesovortices were observed to develop within a narrow 45 km-wide corridor bounded by the apex of the bowing line segment to the south and an east-west thunderstorm outflow boundary to the north.

Numerical simulation studies have increased our understanding of QLCS mesovortex genesis and intensification mechanisms (e.g., Weisman 1993; Weisman and Davis 1998; Trapp and Weisman 2003) and more recently, quasi-idealized numerical simulations by Atkins and Laurent (2009a, b), in addition to observational studies examining Doppler radar characteristics of both tornadic and non-tornadic QLCS mesovortices (e.g., Przybylinski et al. 1996; Atkins and Przybylinski 2000; Atkins et al. 2004; Atkins et al. 2005; Wakimoto et al. 2006b). However, there remains much we do not fully understand as National Weather Service (NWS) operational forecasters continue to struggle in achieving sufficient warning lead times for QLCS tornado events. These struggles are partially a reflection of our limited understanding of the mechanisms associated with QLCS MV genesis and rapid intensification, and inherent limitations of the WSR-88D Doppler radar to adequately sample small-scale, rapidly evolving mesovortices. The 7 August 2013 event presented numerous challenges including rapid QLCS forward propagation speeds, nearly simultaneous genesis and very rapid intensification of several tornadic MVs evolving in close proximity to one another, subsequent complex MV mergers and sparse real-time damage reports at night.

All the tornadic mesovortices evolved within about 35 km from the NWS Green Bay, Wisconsin (KGRB) Doppler radar, thus providing an opportunity to examine these circulations in more detail and hopefully further our understanding of their structure and evolution.

3. SYNOPTIC AND MESOSCALE OVERVIEW

This overview focuses on the synoptic and mesoscale environment during the six-hour period ending at 0500 UTC August 7, 2013 just prior to the height of the tornadic QLCS event.

Scattered strong to severe convection developed over central Minnesota and northwest Wisconsin late in the afternoon of 6 August, and into the early evening of 7 August ahead of a shortwave trough moving across the northern Mississippi Valley (Fig.3).

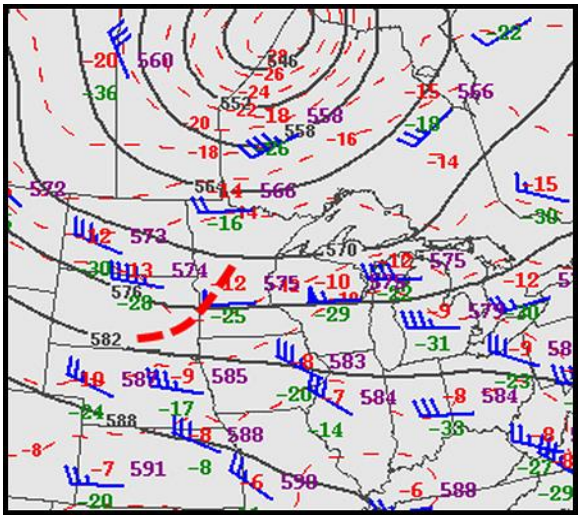

FIG. 3. 00 UTC August 7 500 hPa analysis.

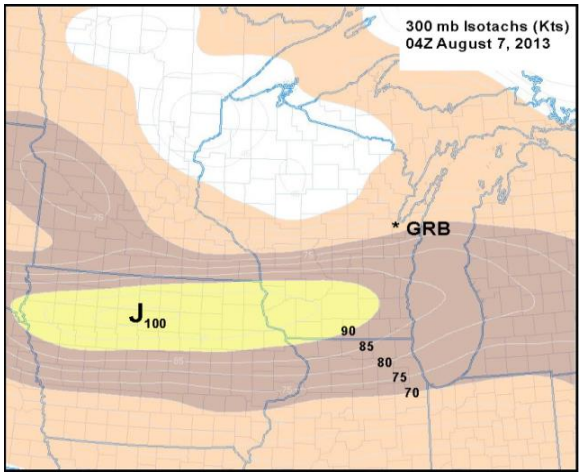

FIG 4. RAP 300 hPa analysis valid 04 UTC August 7

This shortwave was accompanied by a 43 - 49 m s^{-1} jet maximum at 300 hPa which became positioned over Iowa and southern Wisconsin by 0400 UTC (Fig. 4). As the upper trough and jet maximum moved east during the evening, central and east-central Wisconsin became located in an area of increasing upper-level divergence and organized synoptic-scale lift near the left-front quadrant of the upper jet. Mid-level winds were strong reaching speeds of 25 to 28 m s^{-1} which led to 0 to 6 km bulk shear values near 30 m s^{-1} over east-central Wisconsin by 0500 UTC 7 August (not shown). Steep mid-level lapse rates of 7 to 7.5 degrees C km^{-1} pushed into east-central Wisconsin by late evening while at 850 hPa, warm advection was

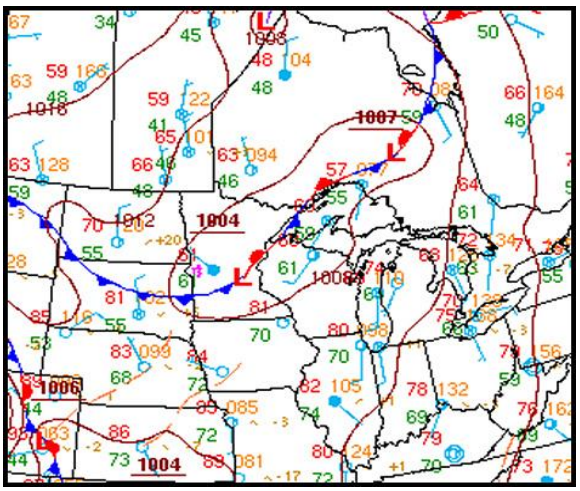

FIG. 5. 00 UTC August 7 surface METAR plot and MSLP (solid lines).

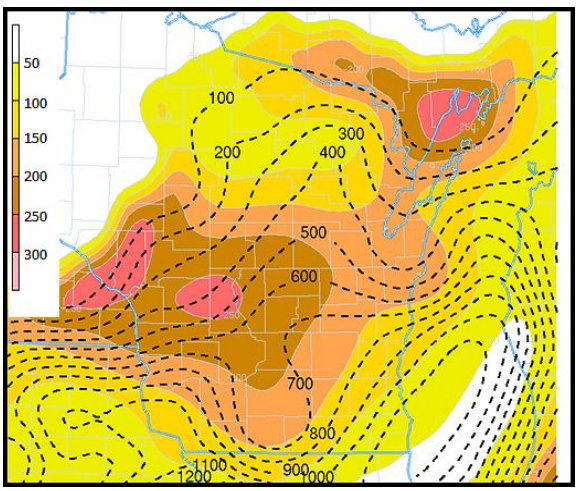

FIG. 7. 05 UTC RAP MLCAPE (dashed) and MLCIN (shaded) analysis.

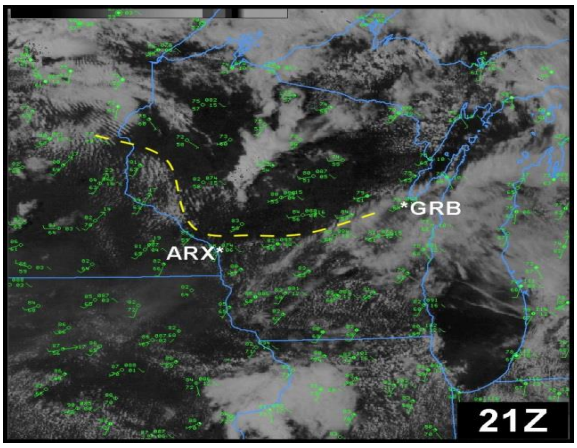

FIG. 6. 21 UTC visible satellite image with surface METAR observations. Dashed line denotes surface moisture discontinuity.

occurring ahead of the shortwave trough. Surface analysis at 0000 UTC 7 August showed low pressure over east-central Minnesota with a stationary front stretching from northwest Wisconsin to northern Ontario, and a cold front extending across southern Minnesota and South Dakota (Fig. 5). A notable moisture discontinuity was also evident over central and east-central Wisconsin by afternoon with surface dewpoints in the middle 50s F to the north and near 70 F to the south of this discontinuity (Fig. 6). As the evening progressed, increasing low-level moisture advection caused surface dewpoints to rebound into the mid to upper 60s F over east-central Wisconsin. Despite the increase in surface moisture during the evening, instability remained modest. By 0500 UTC, the RAP MLCAPE analysis indicated values of 400 to 600 J Kg^{-1} with substantial MLCIN near -200 J Kg^{-1} (Fig. 7). In general, the environment within which the tornadic QLCS evolved could be characterized as a moderate to high shear and low instability environment.

4. QLCS DEVELOPMENT AND INITIAL MESOVORTEX FORMATION

Thunderstorms first developed around 20 UTC 6 August over western Minnesota in the vicinity of a weak surface low and warm front, and in response to destabilization ahead of an approaching upper-level trough. A 26 m s^{-1} westerly mid-level jet advancing into southern Minnesota provided sufficient deep layer shear to support supercells. The primary severe threat associated with this initial discrete convection was large hail and isolated straight-line wind damage. One brief tornado was also reported near the Minnesota-North Dakota border. During the evening, the activity grew upscale and congealed into an extensive quasi-linear convective system that extended across the state of Wisconsin from La Crosse to Marinette as shown in Fig. 8C (lower left image).

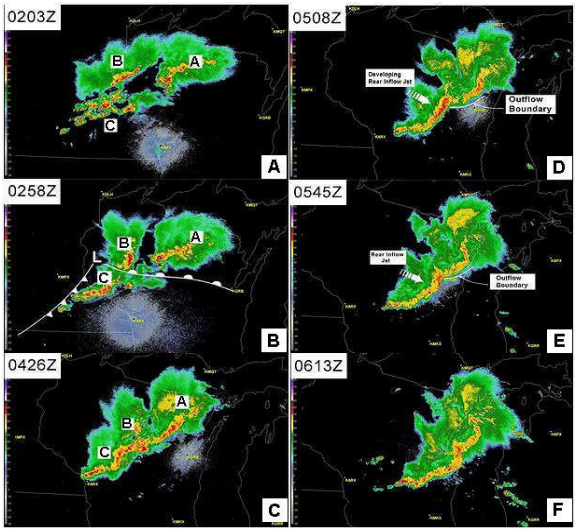

FIG. 8 A-F. Composite radar imagery illustrating evolution of QLCS between 0200 UTC and 0630 UTC 7 August 2013.

Between 0400 UTC and 0430 UTC the southern portion of the QLCS surged eastward becoming orientated nearly N-S across Jackson County (Fig. 8C *denoted by the letter C in white box*). As this portion of the QLCS pivoted to a N-S orientation, several mesovortices quickly formed along the leading edge (Fig. 9). This first episode of mesovortex development occurred in the portion of the QLCS that was most likely in balance and able to maintain more vertically erect updrafts as described by Weisman (1993).

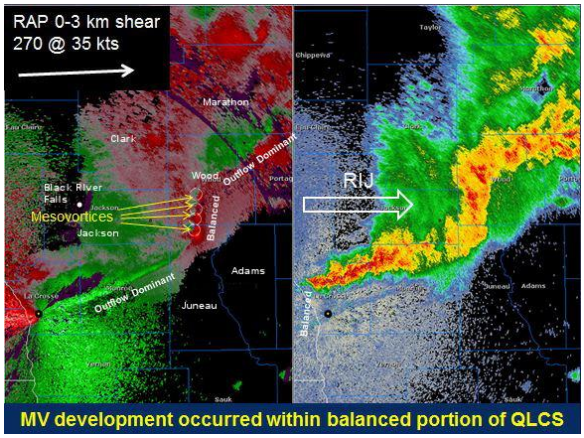

FIG. 9. 0435 UTC Doppler 0.5 degree radar image from KARX. Storm relative velocity is on left and reflectivity is on the right. Mesovortices denoted by the small arrows. Approximate location of rear inflow jet (RIJ) denoted by the large arrow on the reflectivity image.

The RAP 0 to 3 km bulk shear vector analysis valid at 0400 UTC (Fig. 9 insert) indicated the magnitude of the line-normal component of the 0 to 3 km shear immediately downstream of the surging portion of the QLCS approached 18 to 20 ms^{-1}. Schaumann and Przybylinski (2012) have shown that the likelihood for mesovortex genesis tends to increase where 0 to 3 km line-normal bulk shear magnitudes are equal to or greater than 15 m s^{-1} and where a mature rear inflow jet (RIJ) is present. Unfortunately, this first phase of mesovortex development occurred between the KGRB and KARX Doppler radars at distances between 110 km and 130 km, thus the radar sampling was insufficient for detailed analysis of their genesis and evolution. The only known wind damage associated with this initial phase of MV occurrence was with the first mesovortex which formed near Black River Falls (Jackson County) around 0400 UTC. This particular mesovortex was the strongest and most persistent, lasting for nearly two hours producing wind damage shortly after it developed near Black River Falls, and again about 45 minutes later in northern Adams County. As no formal NWS damage surveys were conducted in the area of these initial mesovortices, it is not known with certainty whether any of the wind damage that was reported may have been tornadic in nature. After 0430 UTC, the mesovortices weakened as they continued to move east across Wood County.

5. TORNADIC MESOVORTEX FORMATION

A considerably more intense line surge occurred just north of the initial surge described in the previous section. This subsequent QLCS surge accelerated eastward just south of a nearly quasi-stationary thunderstorm outflow boundary over east-central Wisconsin. This boundary was generated by more outflow-dominant convection located downstream and north of Green Bay, Wisconsin (Fig.10).

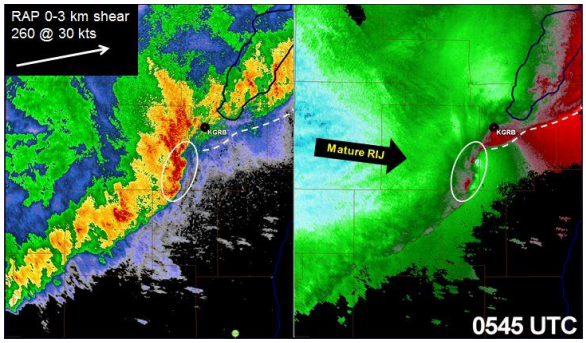

FIG. 10. Same as Fig. 9 except at 0545 UTC. The location of tornadic mesovortices is denoted by the circled area. Approximate location of the thunderstorm outflow boundary is denoted by the dashed white line.

Similar to the first episode of MV development described in the previous section, the mesovortices associated with the second episode formed as the line segment pivoted to a nearly N-S orientation in response to a strong rear inflow jet. This portion of the line also appeared to be nearly in balance, with line-normal 0 to 3 km shear vector magnitudes approaching 15 m s^{-1} based on the 0500 UTC RAP analyses (Fig. 10 insert). All the tornadic MVs formed along the leading edge of the bowing line segment within a 45 km-wide corridor bounded by the outflow boundary to the north and the bow echo apex to the south. The tornadic mesovortices translated eastward at nearly 31 m s^{-1} as they passed within 30 km of the KGRB Doppler radar. As will be shown in the next section, the mesovortices not only formed very quickly, but became tornadic almost immediately following initial genesis in some cases. The rapid mesovortex evolution, in concert with excessive forward propagation speeds, presented an extremely difficult warning decision challenge to forecasters.

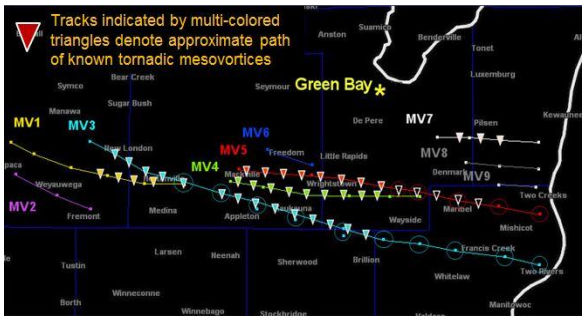

FIG. 11. Preliminary mesovortex tracks associated with the second episode of mesovortex development. Colored triangles denote tornadic mesovortex tracks. Thin circles denote MV tracks following a merger.

6. RADAR ANALYSIS OF THE TORNADIC MESOVORTICES

Careful examination of the KGRB Doppler radar reflectivity and storm-relative velocity data revealed nine mesovortices with the second QLCS line surge (Fig. 11). Six of the mesovortices were determined to be tornadic based on extensive NWS damage assessments in conjunction with detailed analysis of the KGRB Doppler storm-relative velocity and dual-polarization (DP) radar data. Detailed analysis of the dual-polarization differential reflectivity (ZDR) and correlation coefficient (CC) data revealed tornadic debris signatures (TDS) associated with all 6 tornadic mesovortices. The

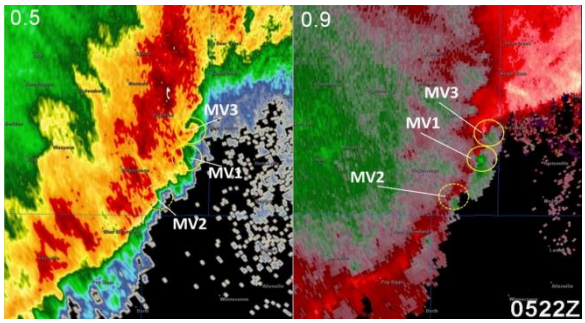

FIG. 12. 0522 UTC radar imagery from KGRB Doppler Radar denoting the location of the first three mesovortices associated with the second QLCS line surge. 0.5 degree reflectivity is on the left and 0.9 degree storm relative velocity is on the right.

criteria used to identify a TDS in the dual-polarization data in this study was similar to that described by Schultz et al. (2012) for S band (10 cm) radars. In order to better understand the relative strength, vertical structure and temporal evolution of the tornadic mesovortices, time-height profiles of MV rotational velocity (Vr) were constructed using storm-relative velocity data from each radar volume scan (VCP212) in a manner similar to that described by Atkins et al. (2005). The estimated maximum height of the TDS was plotted on the time-height traces for comparison. Only time-height traces for the two strongest tornadic mesovortices (MV4 and MV5) will be presented in this paper. The first three mesovortices that developed during the second surge are shown in Fig. 12.

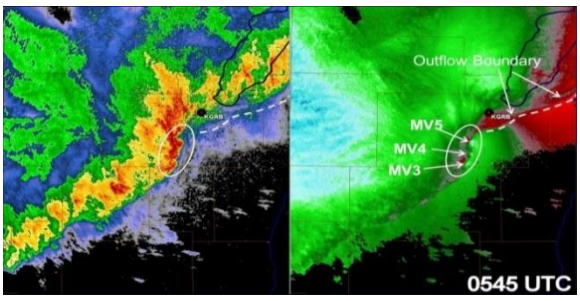

FIG. 13. Same as Fig. 12 except for 0545 UTC. Tornadic MVs denoted by arrows. Approximate location of the thunderstorm outflow boundary is denoted by the dashed white line.

MV1 and MV3 developed quickly with both becoming tornadic within about 2 volume scans (~ 10 minutes) of initial mesovortex genesis. MV2 formed south of the bow apex, was weaker and produced minor non-tornadic wind damage before weakening. Both MV1 and MV3 formed within the balanced portion of the line segment between the bow apex to the south and the east-west outflow boundary to the north. MV1

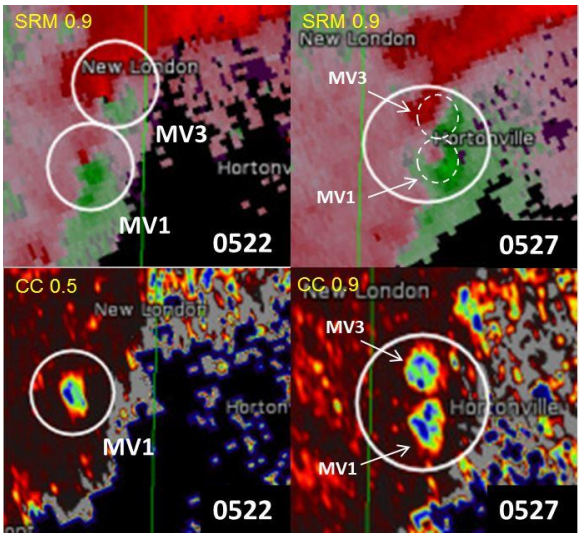

FIG.14. KGRB 4-panel radar display denoted the first two tornadic mesovortices (MV1 and MV3) at 0522 UTC (left) and 0527 UTC (right). Top two images are storm relative velocity at 0.9 degrees. Bottom images are DP correlation coefficient (CC) images at 0.5 and 0.9 degrees.

became tornadic around 0522 UTC and MV3 a few minutes later at approximately 0524 UTC. Maximum Vr values were observed at low-levels (~ 1.5 km) and reached magnitudes of 16 - 18 ms^{-1}. Both MV1 and MV3 generated well-defined TDS signatures as can be seen from the DP correlation coefficient (CC) data in Fig. 14. The TDS associated with MV1 did not appear in the CC radar data until 0527 UTC (lower right-hand panel in Fig. 14). The debris signatures associated with MV1 and MV3 reached maximum heights of ~3.5 km AGL and ~2.5 km AGL, respectively. Based on the formal NWS damage survey, MV3 produced the strongest tornado of the event, briefly reaching EF2 intensity around 0527 UTC near the town of Hortonville, Wisconsin. MV1 merged with MV3 several minutes later with the resultant circulation producing another tornado that reached a maximum intensity of EF1. About 10 minutes later (0538 UTC) the next two tornadic MVs (MV4 and MV5) formed to the north of MV3 and were the most impressive of the tornadic mesovortices in terms of their overall Doppler velocity characteristics (Figs. 13 & 15). MV4 and MV5 evolved close to the KGRB WSR-88D Doppler radar within approximately 30 km. The time-height Vr trace for MV4 is shown in Fig. 17. The trace suggests that tornadogenesis was very rapid occurring almost immediately after the genesis of the mesovortex around 0536 UTC. By the next volume scan (0541 UTC) a TDS signature was noted with MV4 that extended to about 0.7 km (Fig. 16).

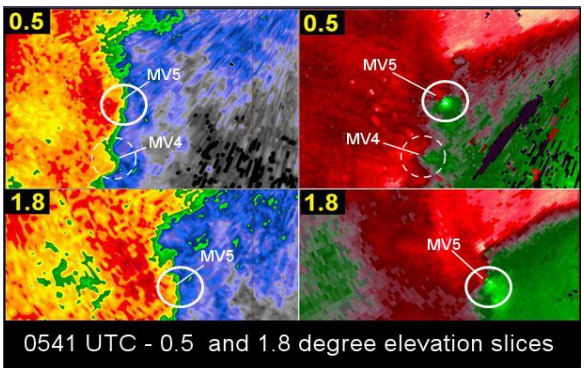

FIG.15. KGRB 4-panel radar display at 0541 UTC denoting tornadic mesovortices MV4 and MV5. Reflectivity is on the left and storm relative velocity is on the right. 0.5 degree elevation slice is on the top and 1.8 degree elevation slice is on the bottom.

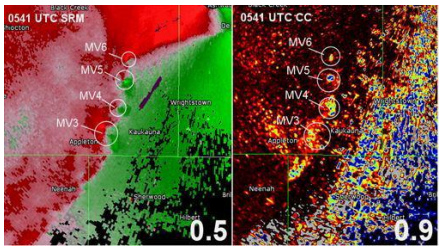

FIG. 16. KGRB 2-panel radar display at 0541 UTC denoting tornadic mesovortices MV4 and MV5 and their associated tornadic debris signatures. The 0.5 degree storm relative velocity is on the left and the 0.9 degree correlation coefficient (CC) is on the right.

It should be noted that it was not obvious whether the TDS observed with MV4 at 0541 UTC (Fig. 16) was exclusively associated with debris lofted by MV4, as residual debris lofted earlier by MV1 and MV3 may have also contributed to the lower CC values.

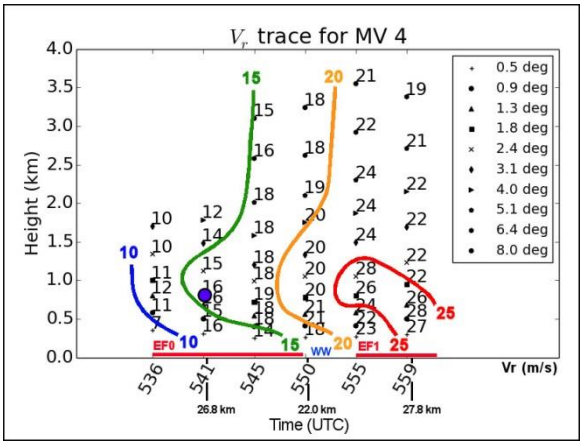

FIG. 17. Time-height rotational velocity (Vr) trace for tornadic mesovortex MV4. Vr values are in m s^{-1}. Y-axis is height (km) and X-axis is the volume scan time (UTC) increasing to the right. The distance (km) from the KGRB radar is also denoted below the volume scan times. Approximate time of tornado on ground denoted by the red line. Blue dot denotes maximum height of the possible TDS at that volume scan time.

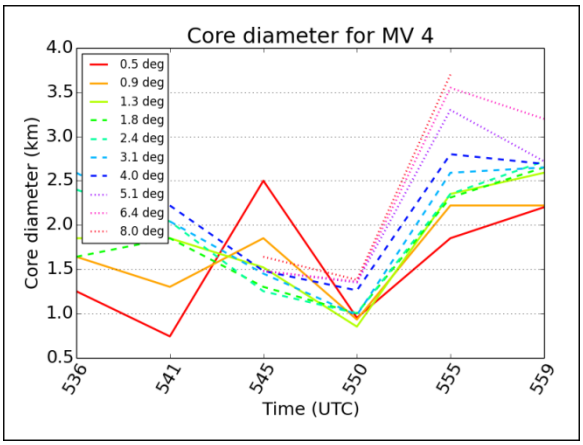

FIG. 18. Time-height trace of MV4 core diameter. Y-axis is core diameter (km) and X-axis is the volume scan time (UTC).

The Vr values associated with MV4 continued to intensify at all levels up to 3.5 km AGL while the low-level mesovortex core diameter decreased to about 1 km by 0550 UTC (Fig. 18). By 0559 UTC, the Vr values reached nearly 28 m s^{-1} between 0.5 and 1.0 km AGL with the tornado reaching its maximum intensity of EF1. After 0559 UTC, MV4 began to interact with MV5 which was located a couple miles to the northwest (Fig. 19). MV5 developed nearly at the same time as MV4 (0536 UTC). The MV5 time-height Vr trace (Fig. 20) reveals very impressive intensification with the circulation reaching a depth of 4 km AGL, while the low-level core diameter decreased to 0.5 km (Fig. 21). In fact, a tornado vortex signature (TVS) was observed in the lowest 4 elevation slices with delta-V values as high as 42 m s^{-1}. A well-defined TDS was also noted (Fig. 16) which reached to nearly 3.0 km AGL (Fig. 20) within one volume scan of MV5 genesis.

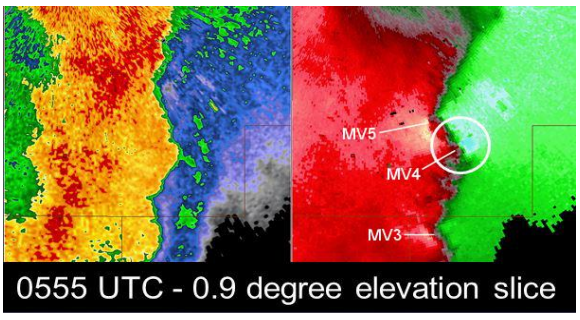

FIG. 19. KGRB 2-panel radar display at 0555 UTC. The 0.9 degree elevation slice. for both reflectivity (left) and storm relative velocity (right) are shown.

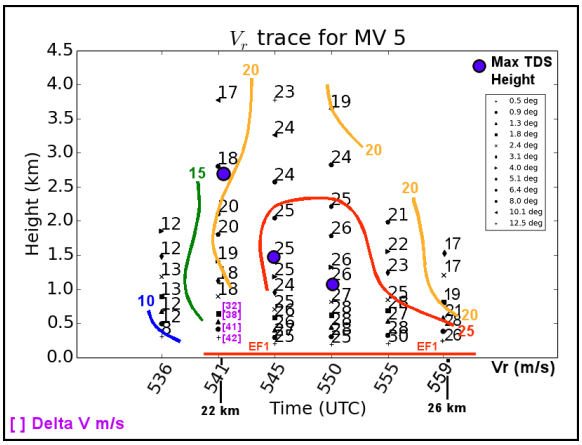

FIG. 20. Same as Fig. 17 except for MV5.

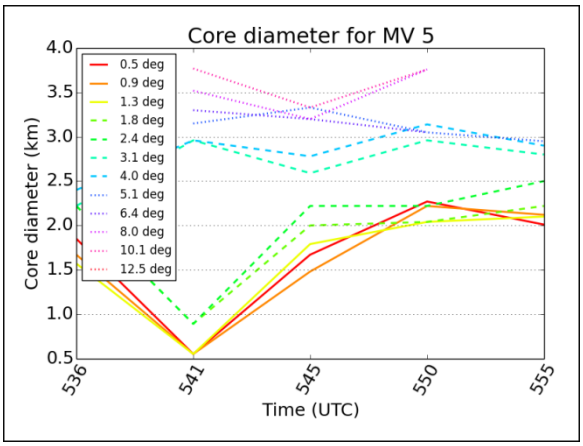

FIG. 21. Same as Fig. 18 except for MV5.

The time-height traces for MV4 and MV5 suggest very rapid vortex stretching along the leading edge of the surging QLCS, with tornadogenesis occurring within about one volume scan of initial MV genesis. This very rapid evolution would provide virtually no opportunity for warning decision makers to issue a tornado warning with any lead time.

7. SUMMARY AND CONCLUSION

A rare early morning tornadic QLCS raced across east-central Wisconsin producing six mesovortex tornadoes within a 45 minute period. The event presented numerous short-term forecast and warning decision challenges to the operational forecasters. As the QLCS was organizing upstream, the short-term forecast challenge centered on uncertainty as to the role a stabilizing nocturnal boundary layer would have on the potential for straight-line wind

damage later on. This uncertainty led to the expectation that sporadic straight-line wind damage would be the primary threat.

There appeared to be two distinct episodes of mesovortex development. In both episodes, mesovortices were observed to form as a portion of the QLCS surged to a more N-S orientation in response to a mature rear inflow jet. This suggests that the surging portion of the line was likely balanced, becoming a favorable location for more vertically erect updrafts that could be more easily stretched. Schaumann and Przybylinski (2012) suggested that line-normal 0 to 3 km bulk shear vector magnitudes in excess of 15 m s^{-1} would favor mesovortex development given a portion of the QLCS line segment was in balance, and where a rear inflow jet or enhanced outflow caused a surge or bow in the line. This three ingredient approach appeared to have some utility in this case and perhaps may have helped forecasters better anticipate mesovortex genesis and subsequent rapid intensification as the QLCS was evolving.

Although it is tempting to speculate as to why the second episode of mesovortex development produced tornadoes while the first episode did not, radar sampling limitations with the first episode precluded a careful and detailed analysis of their genesis and subsequent evolution. Although there were few reports of wind damage associated with the first QLCS line surge, at least one of the mesovortices in the first episode was associated with wind damage. However, it is not known with absolute certainty whether the damage may have been tornadic.

Other interesting aspects of the event that require further study is the role of the east-west thunderstorm outflow boundary that was present during the second tornadic mesovortex phase. All the tornadic mesovortices were observed to occur between the apex of the bow to the south and the thunderstorm outflow boundary to the north. In fact, the strongest mesovortex (MV5) evolved very near or just south of this boundary. Although not discussed earlier, a substantially weaker mesovortex (MV6) was also observed to form on the boundary (Figs. 15 & 16) just to the north and around the same time as MV5 (0536 UTC). There is evidence that MV6 may have merged with MV5 around the same time the TVS signature was observed with MV5, around 0541 UTC. However, this preliminary observation should be considered tenuous, given the fast forward propagation and very rapid MV evolution that likely occurred between consecutive volume scans.

Based on the RAP MLCIN analysis immediately upstream from the tornadic QLCS, there appeared to be a surface-based stable layer present. Based on the Vr trace associated with the most impressive tornadic mesovortex (MV5) and its associated tornado vortex signature (TVS), it was somewhat surprising that only EF1 intensity damage was observed. More research needs to be done to better understand the potential impact of stable boundary layers on QLCS tornadogenesis, as well as the impact of low theta-e air situated immediately behind the leading gust front.

Finally, although not the focus of this paper, several mesovortex tornado debris signatures (TDS) were observed. Debris signatures associated with QLCS tornadoes have not been observed as readily compared to those associated with supercell tornadoes and thus, require further study. The TDS signatures in this case were very transient and sometimes extremely difficult to identify and track from one volume scan to the next. This was due to several factors including, the rapid forward propagation of the QLCS, the small size and very rapid evolution of the tornadic MVs, the very close proximity of the MVs to one another, and subsequent tornadic MV mergers. Also, as shown in Fig. 16, there was evidence of a brief (one volume scan) TDS-like signature associated with MV6, however there was no known damage associated with this feature. Broader debris-like signatures (i.e., broad areas of relatively low CC) were noted along and immediately behind the leading gust front, particularly during the latter stages of the event. It is speculated that these broader areas of relatively low-CC may be the result of biomass (e.g., leaves, twigs, dust) lofted along the leading QLCS gust front which had accelerated to nearly 31 ms^{-1} before moving out over Lake Michigan.

Acknowledgements. Thanks to Mike Cellitti and Scott Berschback for their assistance in the analysis of the synoptic and mesoscale environment. Jason Schaumann for enthusiastically sharing valuable insight regarding this case and Laura Kanofsky for generating the time-height velocity and core diameter traces.

References

Atkins, N.T., J.M. Arnott, R.W. Przybylinski, R.A. Wolf, and B.D. Ketcham, 2004: Vortex structure and evolution within bow echoes. Part I: Single-Doppler and damage analysis of the 29 June 1998 derecho. *Mon. Wea. Rev*., **132**, 2224-2242.

Atkins, N.T., C.S. Bouchard, R.W. Przybylinski, R.J. Trapp, and G. Schmocker, 2005: Damaging surface wind mechanism within the 10 June 2003 Saint Louis bow echo during BAMEX. *Mon. Wea. Rev*., **133**, 2275-2296.

.

Atkins, N.T., and M. St. Laurent, 2009a: Bow echo mesovortices. Part I: Processes that influence their damaging wind potential. *Mon. Wea. Rev*., **137**, 1497-1513.

Atkins, N.T., and M. St. Laurent, 2009b: Bow echo mesovortices. Part II: Their Genesis. *Mon. Wea. Rev*., **137**, 1514-1532.

Atkins, N.T., and R.W. Przybylinski, 2000: Radar and damage analysis of the 27 May 2000 tornadic derecho event. *Preprints, 21st Conf. on Severe Local Storms*, San Antonio, TX, *Amer. Meteor. Soc*. 567-570.

Kis, A.K., and J.M. Straka, 2009: Nocturnal Tornado Climatology. *Wea. Forecasting,* **25**, 545-561.

Przybylinski, R.W, Y.J. Lin, C.A. Doswell III, GK. Schmocker, T. J. Shea, T.W. Funk, K.E. Darmofal, J.D. Kirkpatrick, and M.T. Shields, 1996: Storm reflectivity and mesocyclone evolution associated with the 15 April 1994 derecho, Part I: Storm structure and evolution over Missouri and Illinois. *Preprints, 18th Conf. on Severe Local Storms*, San Francisco, CA, *Amer. Meteor. Soc*., 509-515.

Schaumann, J.S., and R.W. Przybylinski, 2012: Operational Application of 0-3 km bulk shear vectors in assessment of QLCS mesovortex and tornado potential. *Preprints 26th Conf. on Severe Local Storms*, Nashville, TN, *Amer. Meteor. Soc*., P9.10.

Schultz, C.J., Carey, E.V. Schultz, B.C. Carcione, C.B. Darden, C.C Crowe, P.N. Gatlin, D.J. Nadler, W.A. Petersen, and K.R. Knupp, 2012: Dual-polarization tornadic debris signatures. Part I: Examples and utility in an operational setting. *Electronic J. Operational Meteor*., **13**(9), 120-137.

Trapp, R.J., and M.L. Weisman, 2003: Low-level mesovortices within squall lines and bow echoes. Part II: Their genesis and implications. *Mon. Wea. Rev,* **131***,* 2804-2823*.*

Wakimoto, R. M., C.A. Davis, and N.T. Atkins, 2006b: High winds generated by bow echoes. Part II: The relationship between the mesovortices and damaging straight-line winds*. Mon Wea. Rev*., **134**, 2813-2829.

Weisman, M. L., 1993: The genesis of severe, long-lived bow echoes. *J. Atmos. Sci*., **50**, 645-670.

___, and C. Davis, 1998: Mechanisms for the generation of mesoscale vortices within quasi-linear convective systems. *J. Atmos. Sci.,* **55**, 2603-2622.